

## Antitumor Agents

How to cite:

International Edition: doi.org/10.1002/anie.202102266

German Edition: doi.org/10.1002/ange.202102266

## Interfering with Metabolic Profile of Triple-Negative Breast Cancers Using Rationally Designed Metformin Prodrugs

Maria V. Babak,\* Kai Ren Chong, Peter Rapta, Markella Zannikou, Hui Min Tang, Lisa Reichert, Meng Rui Chang, Vladimir Kushnarev, Petra Heffeter, Samuel M. Meier-Menches, Zhi Chiaw Lim, Jian Yu Yap, Angela Casini, Irina V. Balyasnikova, and Wee Han Ang\*

**Abstract:** Triple-negative breast cancer (TNBC) is the most aggressive subtype of breast cancer, characterized by an aberrant metabolic phenotype with high metastatic capacity, resulting in poor patient prognoses and low survival rates. We designed a series of novel Au<sup>III</sup> cyclometalated prodrugs of energy-disrupting Type II antidiabetic drugs namely, metformin and phenformin. Prodrug activation and release of the metformin ligand was achieved by tuning the cyclometalated Au<sup>III</sup> fragment. The lead complex **3met** was 6000-fold more cytotoxic compared to uncoordinated metformin and significantly reduced tumor burden in mice with aggressive breast cancers with lymphocytic infiltration into tumor tissues. These effects were ascribed to **3met** interfering with energy production in TNBCs and inhibiting associated pro-survival responses to induce deadly metabolic catastrophe.

## Introduction

Metformin and its less polar analogue phenformin belong to a family of biguanides (Figure 1A) that are widely prescribed as over-the-counter antidiabetic medications. Metformin in particular is a first-line treatment for Type II diabetes and listed as one of World Health Organization (WHO) essential medicines.<sup>[1]</sup> While there is a substantial evidence of the association between diabetes and increased cancer risk, retrospective epidemiological analyses revealed that diabetic patients taking metformin or phenformin for prolonged periods have significantly reduced cancer incidence.<sup>[2]</sup>

The anticancer activity of metformin and phenformin has been linked to their ability to alter cancer cell metabolism.<sup>[3]</sup> Cancer cells progressively modify normal cellular functions in order to promote rapid proliferation and disable cell death mechanisms and immune surveillance.<sup>[4]</sup> Acceleration of normal cell division requires metabolic adjustments to provide cancer cells with the additional energy; hence, they switch their main energy production from the oxidative phosphorylation (OXPHOS) to the less efficient aerobic glycolysis. However, the loss of ATP is counterbalanced by a higher glycolytic rate and increased glucose uptake. Since constant energy supply is paramount to cancer cells' survival,<sup>[5]</sup> the interference with their energy production results in a metabolic catastrophe which inevitably leads to cancer cell death.<sup>[6]</sup> Metformin and phenformin target energy production in cancer cells by inhibiting Complex I of the mitochondrial respiratory chain,<sup>[7]</sup> activating 5'-adenosine monophosphate-activated protein kinase (AMPK)<sup>[8]</sup> and lowering body insulin levels by altering insulin/insulin-like growth factor-I (I/IGF) pathway.<sup>[2a,5b]</sup> In addition, metformin and phenformin have been repeatedly shown to enhance antiproliferative effects of other drugs, including cisplatin,<sup>[9]</sup> 2-deoxyglucose,<sup>[10]</sup> doxorubicin<sup>[11]</sup> and tamoxifen<sup>[12]</sup> in a synergistic manner both in vitro and in vivo.<sup>[2a,13]</sup>

Despite the well-characterized anticancer effects<sup>[2a]</sup> and low cost, the use of metformin as an anticancer agent features serious drawbacks. According to the Biopharmaceutics Classification System (BCS) and Biopharmaceutics Drug Disposition Classification System (BDDCS), metformin is classified

[\*] Dr. M. V. Babak

Drug Discovery Lab, Department of Chemistry  
City University of Hong Kong  
83 Tat Chee Avenue, 999077 Hong Kong SAR (P. R. China)  
E-mail: mbabak@cityu.edu.hk

K. R. Chong, H. M. Tang, L. Reichert, M. R. Chang, Z. C. Lim,  
Dr. J. Y. Yap, Prof. W. H. Ang  
Department of Chemistry, National University of Singapore  
3 Science Drive 2, 117543 Singapore (Singapore)  
E-mail: chmawh@nus.edu.sg

Prof. P. Rapta  
Institute of Physical Chemistry and Chemistry Physics  
Slovak Technical University of Technology  
Radlinského 9, 82137 Bratislava (Slovak Republic)

Dr. M. Zannikou, Prof. I. V. Balyasnikova  
Department of Neurological Surgery  
The Feinberg School of Medicine, Northwestern University  
Chicago, IL 60611 (USA)

Dr. V. Kushnarev

FSBI "National Medical Research Center of Oncology, named after N.N. Petrov", Ministry of Healthcare of the Russian Federation  
68 Leningradskaya Street, Pesochny, 197758 St Petersburg (Russian Federation)

Prof. P. Heffeter  
Institute of Cancer Research and Comprehensive Cancer Center,  
Department of Medicine I, Medical University of Vienna  
Borschkegasse 8a, 1090 Vienna (Austria)

Dr. S. M. Meier-Menches  
Department of Analytical Chemistry, Faculty of Chemistry  
University of Vienna, Vienna (Austria)

Prof. A. Casini  
Department of Chemistry, Technical University of Munich  
Lichtenbergstr. 4, 85748 Garching, München (Germany)

 Supporting information and the ORCID identification number(s) for the author(s) of this article can be found under:  
<https://doi.org/10.1002/anie.202102266>

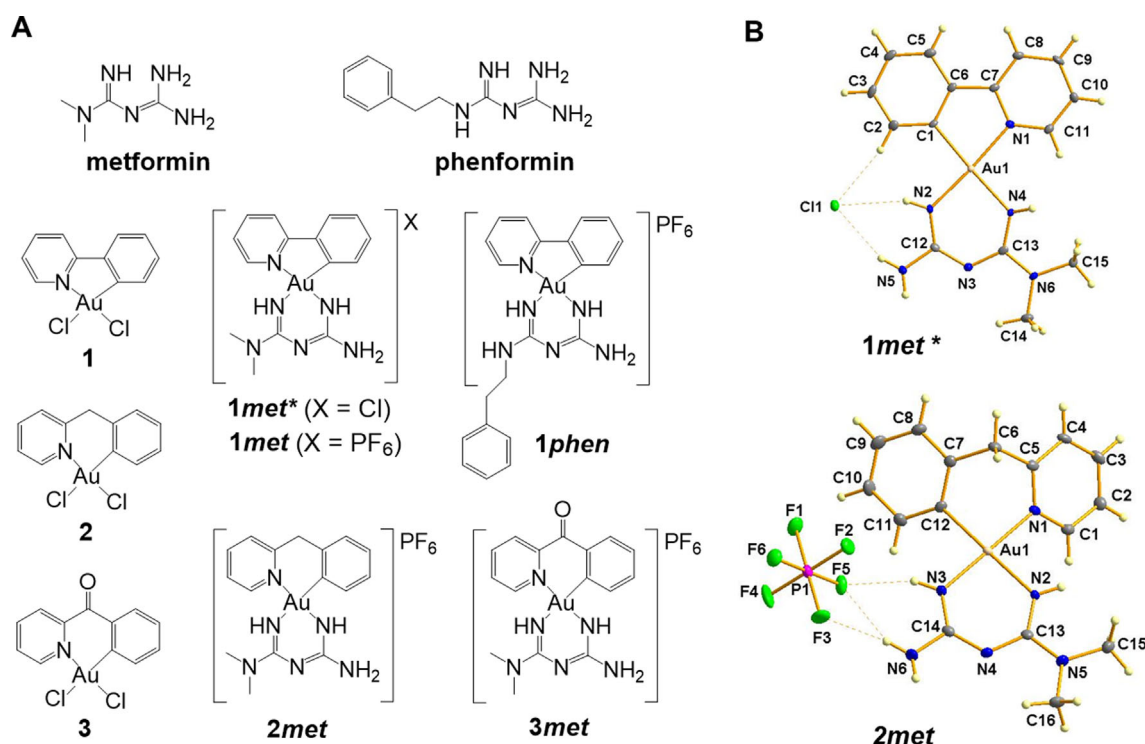


**Figure 1.** Cyclometalated Au<sup>III</sup> complexes of interest. A) Chemical structures of metformin, phenformin and Au<sup>III</sup> complexes used in this study. B) ORTEP representation of **1met\*** and **2met**; non-H atoms are represented as thermal ellipsoids at 50% probability; solvent molecules were omitted for clarity.

as a Class 3 compound, indicating its hydrophilic character and low permeability across cellular membranes at physiological pH.<sup>[14]</sup> Due to poor cellular uptake, its anticancer effects in vitro were observed only at high millimolar concentrations. Similarly in cancer patients, metformin and phenformin demonstrated anticancer effects only when taken repeatedly in high doses, which might cause significant side-effects.<sup>[15]</sup> In fact, high doses of phenformin induced fatal lactic acidosis leading to its withdrawal from the market.<sup>[16]</sup> To overcome the difficulties associated with conventional high dosages of metformin and phenformin, various strategies have been employed. Encapsulation of these drugs into delivery systems significantly improved their delivery into cancer cells leading to reduced side effects.<sup>[17]</sup> Conjugation of metformin with mitochondria-targeting triphenylphosphonium cation resulted in a marked increase of in vitro cytotoxicity up to low micromolar range.<sup>[18]</sup> Additionally, several organic prodrugs of metformin have been prepared, which improved the oral availability of the drug.<sup>[19]</sup> However, the chemical conjugation of metformin and phenformin with another active pharmacophore has never been explored so far.

In this work, we prepared five novel rationally designed organometallic Au<sup>III</sup>-metformin and phenformin complexes (**1–3met**, **1phen**, and **1met\***) based on three different cyclometalated fragments featuring bidentate C<sup>^</sup>N type of ligands (Figure 1A) which were shown to release metformin and phenformin in cancer cells and demonstrated excellent activity in vitro. The lead complex **3met** was more than 6000-fold more active than metformin and demonstrated

excellent in vivo efficacy in highly tumorigenic breast cancer tumors with TNBC phenotype.

## Results

Our design strategy was centered on novel metformin and phenformin prodrugs which would (i) release these drugs and other active species inside cancer cells and (ii) ensure synergistic anticancer action of both pharmacophores. Therefore, we exploited a prodrug strategy where metformin and phenformin were incorporated into cyclometalated Au<sup>III</sup> scaffolds featuring bidentate C<sup>^</sup>N ligands. In general, in the hypoxic conditions of cancer cells, Au<sup>III</sup> complexes of this type were activated either by reduction or ligand substitution mechanisms and exhibited excellent anticancer activity in vitro and in vivo.<sup>[20]</sup> Compounds of this family were shown to target selected zinc-finger domains, protein tyrosine phosphatases (PTP) and thioredoxin reductase (TrxR) enzymes, thereby altering normal mitochondrial function.<sup>[21,22]</sup> Since both metformin and Au<sup>III</sup> fragments were shown to affect mitochondria by interfering with different pathways, we hypothesized that chemical attachment of metformin and phenformin to a Au<sup>III</sup> center would ensure the complementary action of both fragments in cancer cells.

Cyclometalated Au<sup>III</sup> complexes with metformin or phenformin were prepared starting from Au<sup>III</sup>-dichlorido precursors with the general formula [Au<sup>III</sup>(C<sup>^</sup>N)Cl<sub>2</sub>] **1–3** (C<sup>^</sup>N = 2-phenylpyridine (**1**), 2-benzylpyridine (**2**) and 2-benzoylpyridine (**3**)). The synthesis was adapted from Che et al.<sup>[23]</sup>

Precursors **1–3** were synthesized from  $\text{KAuCl}_4$  under microwave conditions or by reflux with  $\text{AgOTf}$  and subsequently reacted with 2 equiv. of metformin or phenformin hydrochloride in methanol (Supporting Information, Scheme S1). 4 equiv. of  $t\text{BuOK}$  were added into reaction mixture to facilitate the coordination of biguanide ligand to  $\text{Au}^{\text{III}}$ . Complexes **1–3met** and **1phen** were isolated as  $\text{PF}_6^-$  salts in moderate yields after counter-ion exchange with  $\text{NH}_4\text{PF}_6$ . These complexes were lowly soluble in water and highly soluble in DMSO. Additionally,  $\text{Au}^{\text{III}}$ -metformin complex with 2-phenylpyridine **1mer\*** was isolated as a  $\text{Cl}^-$  salt by taking advantage of its relatively poor solubility in methanol and all other organic solvents, resulting in direct precipitation from the reaction media. Upon coordination of the asymmetric metformin or phenformin to a  $\text{Au}^{\text{III}}$  center, complexes formed racemic mixtures of *E*- and *Z*- isomers, as evidenced by two independent sets of  $^1\text{H NMR}$  signals. Detailed synthesis and characterization of  $\text{Au}^{\text{III}}$  complexes are presented in the Supporting Information, Figures S1–S23. Purity was assessed by RP-HPLC or elemental analysis and shown to be > 98% pure for all complexes (Supporting Information, Figures S13–S19). The solid-state structures of **1mer\*** and **2met** were analyzed by X-ray diffraction analysis (Figure 1 B; Supporting Information, Tables S1,S2).

The stability of  $\text{Au}^{\text{III}}$  complexes in  $[\text{D}_6]\text{DMSO}$  was assessed by  $^1\text{H NMR}$  spectroscopy over 10 d (Supporting Information, Figures S10–S12). To determine the speciation of the  $\text{Au}^{\text{III}}$  complexes in aqueous solution, the compounds were incubated in ammonium carbonate buffer (pH 7.4) at  $37^\circ\text{C}$  for 1, 3 and 24 h and analyzed by high resolution ESI-MS.<sup>[24]</sup> Compounds **1–3met** were stable for 24 h as evidenced by the detection of molecular ions  $[\text{M}]^+$  (Supporting Information, Table S3 and Figure S24). Conversely, the  $[\text{M}]^+$  signal for **1phen** was not detected after 1 h incubation, indicating lower stability in comparison with the other  $\text{Au}^{\text{III}}$ -metformin analogues (Supporting Information, Figure S25). Furthermore, when **1phen** was incubated in the presence of 1 equiv. of glutathione (GSH) for the same time period, the release of phenformin was detected at  $206.1622\text{ m/z}$ , which was not observed in the absence of GSH (Supporting Information, Figures S26 and S27). Intriguingly, the reactivity of  $\text{Au}^{\text{III}}$ -metformin complexes towards GSH was drastically different despite their similar structures. **3met** demonstrated time-dependent release of metformin characterized by evident optical changes in UV/Vis spectrum and appearance of the new peak at 235 nm corresponding to free metformin (Figure 2 A). Similarly, when metformin release was monitored by ESI-MS, an increase of the metformin signal at  $130.1078\text{ m/z}$  and significant decrease of  $[\text{M}]^+$  signal at  $506.1358\text{ m/z}$  were observed (Supporting Information, Figures S28–S30). On the contrary, **1met** demonstrated metformin release only upon heating (Supporting Information, Figure S32), while **2met** exhibited good stability both in the absence and presence of GSH (Figure 2 B; Supporting Information, Figure S31). Recent studies showed that a  $\text{Au}^{\text{III}}$  complex featuring 2-benzoylpyridine scaffold efficiently arylated GSH via a reductive elimination process, in agreement with enhanced reactivity of **3met**.<sup>[25]</sup>

To determine whether the release of metformin occurred as a result of electrochemical reduction of  $\text{Au}^{\text{III}}$ , we performed cyclic voltammetry experiments in DMSO or aqueous solution (Figure 2 C). While uncoordinated metformin did not show any redox activity, the cyclic voltammograms of **1–3met** and **1phen** demonstrated a reduction wave in the cathodic region at  $-0.6$  to  $-1.1\text{ V}$  (vs. NHE), corresponding to an irreversible reduction of  $\text{Au}^{\text{III}}$  to  $\text{Au}^{\text{I}}$ . However, the redox potentials were outside accessible biological window, indicating that direct reduction of  $\text{Au}^{\text{III}}$  in cancer cells was unlikely. Subsequently, cyclic voltammetry measurements were coupled with UV/Vis in a spectroelectrochemical cell, which revealed that cathodic reduction of  $\text{Au}^{\text{III}}$  in **1met** and **3met**, but not **2met**, was associated with the appearance of new transitions in the region between 350 and 600 nm (Figure 2 D; Supporting Information, Figures S33 and S34). Taken together, the interaction of  $\text{Au}^{\text{III}}$  complexes with GSH might be considered as a competition between reduction and ligand substitution; however, we suggest that the latter occurred prior to reduction, in agreement with the literature.<sup>[20a]</sup> In the case of **3met**, further gold-templated C-S cross coupling can also be hypothesized.<sup>[25]</sup>

The  $\text{Au}^{\text{III}}$  complexes were tested against the aggressive poorly differentiated TNBC cell line, MDA-MB-231, as well as other human cancer cell lines, and exhibited high cytotoxicities in all cases (Supporting Information, Table S4, Figure S35). In contrast, metformin was devoid of cytotoxicity, while phenformin was only marginally cytotoxic, in agreement with the literature.<sup>[23,24,26]</sup> In keeping with reduced stability, **1phen** was the least cytotoxic representative of this series. Additionally, we assessed the compounds' toxicity in human ventricular cardiomyocytes (AC10) in comparison with doxorubicin, which is severely cardiotoxic, as a control (Supporting Information, Table S4). The heart toxicity of doxorubicin in AC10 cells was reflected by the  $\text{IC}_{50}$  value  $2.3 \pm 0.2\ \mu\text{M}$ , whereas cisplatin and **3met** were approximately 3–4-fold less toxic. All other  $\text{Au}^{\text{III}}$  complexes were only marginally toxic or non-toxic at all. Similar results were observed upon assessment of the liver toxicity using mouse hepatocytes (TAMH) (Supporting Information, Table S4). It should be noted that **3met**, while being more toxic than other structurally similar complexes, demonstrated 4-fold selectivity to liver cells over resistant MDA-MB-231 cancer cells.

The differences in cytotoxicity of  $\text{Au}^{\text{III}}$  complexes might be related to their intracellular accumulation. Therefore, we determined the intracellular Au content in MDA-MB-231 cells by ICP-MS upon exposure to increasing concentrations of compounds for 24 h (Supporting Information, Table S4 and Figure S36). All complexes demonstrated concentration-dependent cellular accumulation with the highest accumulation for **3met**, in agreement with its highest cytotoxicity. Subsequently, we determined whether  $\text{Au}^{\text{III}}$  complexes and metformin induced apoptosis at their respective  $\text{IC}_{50}$  values by using the Annexin V/PI assay (Supporting Information, Figure S37A). All complexes showed significantly higher increase of apoptotic cell population than metformin or cisplatin after 24 h treatment and apoptosis was not affected by the variation of cyclometalated or biguanide fragments in **1–3met** and **1phen**. These results indicated that all complexes

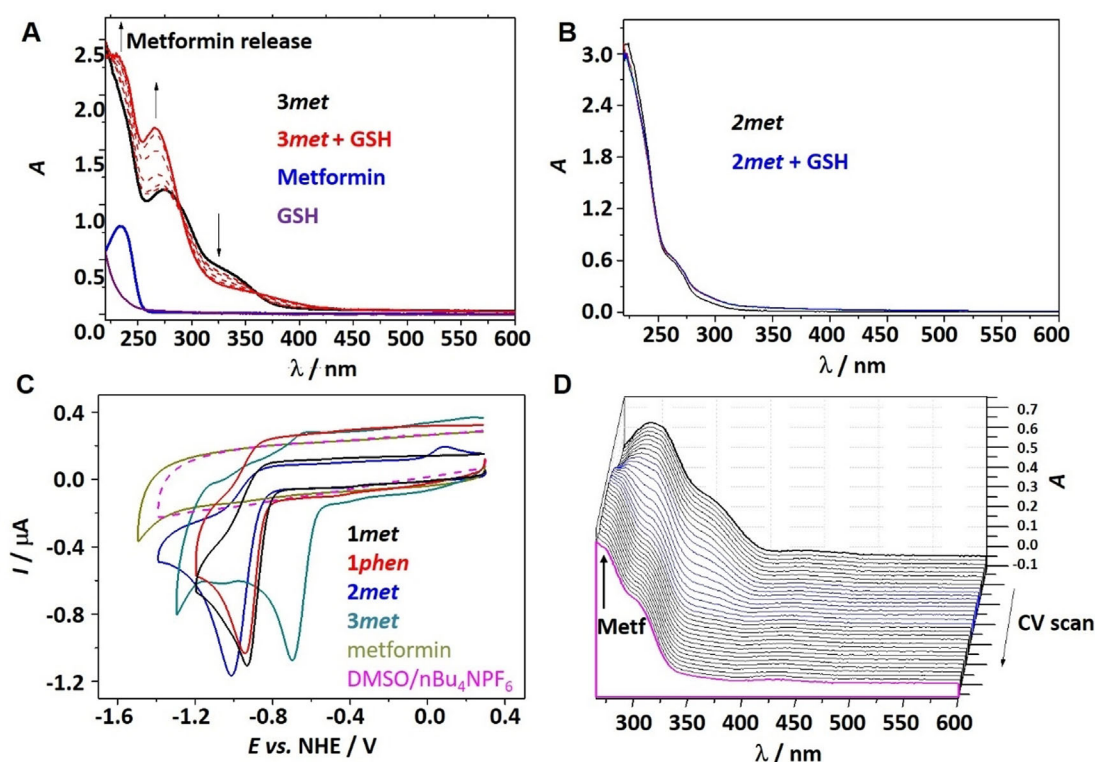


**Figure 2.** Reactivity with GSH and redox properties. A) Changes in the UV/Vis spectra of **3met** in water at pH7 upon sequential addition (6 times) of 0.4 equiv. of glutathione (GSH) in comparison with spectra of GSH and metformin. B) Changes in the UV/Vis spectra of **2met** in water at pH 7 upon sequential addition (6 times) of 0.4 equiv. of GSH. C) Cyclic voltammograms of Au<sup>III</sup>-metformin and phenformin complexes and uncoordinated metformin in DMSO/*n*Bu<sub>4</sub>NPF<sub>6</sub> at potential scan rate of 100 mV s<sup>-1</sup>. D) Changes in UV/Vis spectra (scan rate 10 mV s<sup>-1</sup>) upon cyclic voltammetry forward scan for **3met** in DMSO/*n*Bu<sub>4</sub>NPF<sub>6</sub> (thick black line: initial spectrum, blue lines optical changes in the region of the first irreversible cathodic peak, magenta line: final UV/Vis spectrum after re-oxidation).

induced equal levels of apoptosis when treated at equipotent concentrations. We further monitored cleavage of poly(ADP-ribose)polymerase-1 (PARP) and caspase-3 in treated cells, hallmarks of apoptotic cell death, and compared the cytotoxicity of **3met** in presence or absence of poly-caspase inhibitor Z-VAD-FMK (Supporting Information, Figures S37B and S38). The cytotoxicity significantly decreased when cells were co-treated with Z-VAD-FMK, while dose- and time-dependent cleavage of PARP and caspase-3 were observed, suggesting that Au<sup>III</sup>-metformin complexes exerted mitochondrial caspase 3-dependent apoptosis *in vitro*.

Since the mechanism of cyclometalated Au<sup>III</sup> complexes in cancer cells commonly involved the inhibition of thioredoxin reductase (TrxR), we investigated the TrxR-inhibitory potential of **1-3met**, **1phen** and metformin (Supporting Information, Table S4, Figure S39). As expected, all tested complexes demonstrated comparable nanomolar inhibitory activity (IC<sub>50</sub> ≈ 0.5–3 nM) against rat liver TrxR. In contrast, uncoordinated metformin did not show any inhibitory potential up to 5 mM; therefore, TrxR-inhibitory potential of Au<sup>III</sup>-metformin complexes was attributed to a Au<sup>III</sup> moiety. Inhibition of mitochondrial TrxR may trigger various antimitochondrial effects, leading to the defective mitochondrial respiration and energy metabolism.<sup>[27]</sup> We therefore investigated the effects of **3met** on mitochondrial OXPHOS system of MDA-MB-231 cells (Figure 3 A; Supporting Information, Figure S40A) us-

ing the Seahorse Mitostress assay. **3met** demonstrated dose-dependent progressive decrease of all mitochondrial bioenergetic parameters, indicating inhibition of mitochondrial processes and loss of mitochondrial mass, similar to other mitochondria-targeting metal-based complexes.<sup>[22b,28]</sup> In contrast, non-mitochondrial respiration of cancer cells was not significantly inhibited (Figure 3 A). Since the loss of ATP in cancer cells was counterbalanced by an increased glycolytic rate,<sup>[3]</sup> we analyzed the glycolytic function of MDA-MB-231 cells treated with increasing concentrations of **3met** (Figure 3 B; Supporting Information, Figure S40B). Cancer cells displayed elevated aerobic glycolysis upon exposure to low concentrations of **3met** (0.05 μM) for 24 h. However, treatment of cancer cells with higher concentration of **3met** resulted in their declined glycolytic function. These results indicated the attempts of cancer cells to confer a survival advantage in presence of **3met** by greater compensatory increase in aerobic glycolysis.

One of the main mechanisms, by which metformin alters mitochondrial energy metabolism and function in cancer cells, involves the interference with AMPK and mTOR pathways, which regulate the energetic balance at the whole body level.<sup>[29]</sup> When MDA-MB-231 cells were treated with increasing concentrations of **1met** and **3met** for 24 h, the increase of AMPK phosphorylation and decrease of mTOR phosphorylation was detected similar to high concentrations of



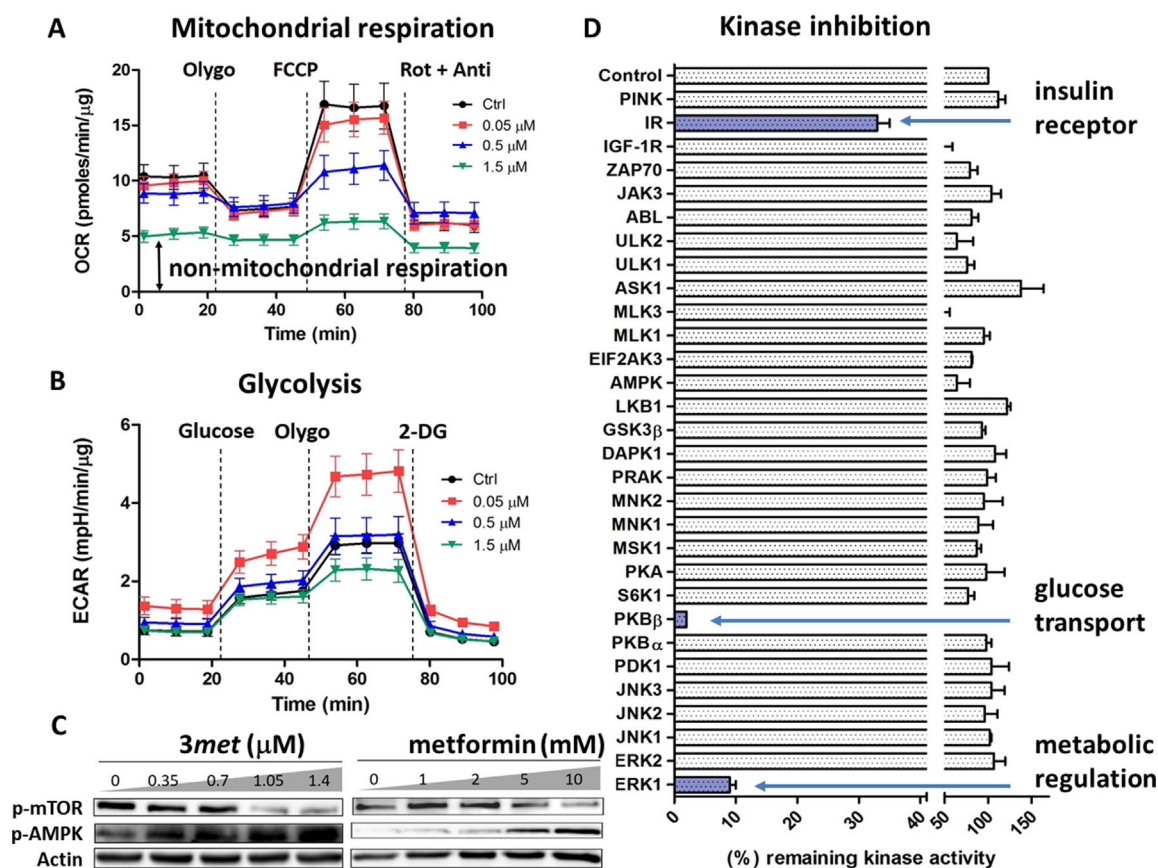


**Figure 3.** Potent energy disruption. A) Mitochondrial respiration characterized by oxygen consumption rate (OCR) upon sequential addition of oligomycin, carbonyl cyanide-4-(trifluoromethoxy)phenylhydrazone (FCCP) and rotenone with antimycin, normalized by protein content in MDA-MB-231 cells treated with **3met** for 24 h at indicated concentrations. B) Glycolysis characterized by extracellular acidification rate (ECAR) upon sequential addition of glucose, oligomycin and 2-deoxyglucose, normalized by protein content in MDA-MB-231 cells treated with **3met** for 24 h at indicated concentrations. C) Western blot analysis of p-mTOR and p-AMPK involved in bioenergetics of MDA-MB-231 cells treated with **3met** and metformin or 24 h at indicated concentrations. D) Remaining kinase activity (%) after 24 h co-incubation with 10  $\mu$ M of **3met**.

uncoordinated metformin (Figure 3C; Supporting Information, Figure S41). mTOR undergoes phosphorylation when growth conditions are favorable. Unlike mTOR however, phosphorylation of AMPK indicates activation of AMPK followed by mTOR inhibition, thereby supporting the observed effects of the complexes on the mitochondrial respiration. The inhibition of cancer metabolism induced by **3met** might be related to the inhibition of kinases, involved in the energy regulation processes. Therefore, we determined the residual in vitro activity of 30 relevant kinases upon incubation with **3met** (Figure 3D). The analysis revealed that **3met** was a relatively specific inhibitor, targeting extracellular signal-regulated kinase 1 (ERK1), protein kinase B beta (PKB $\beta$ ) and insulin receptor (IR) kinases which played key roles in the metabolic function of cancer cells. This was in keeping with previous reports that metformin was also involved in PKB, ERK and IR signalling.<sup>[2a,30]</sup>

The major role in restoring normal cellular function under stressful conditions is mediated by unfolded protein response (UPR) and autophagy, which are activated in response to the accumulation of unfolded or misfolded proteins in the endoplasmic reticulum (ER).<sup>[31]</sup> **3met** was able to induce pro-survival UPR activation in MDA-MB-231 cells charac-

terized by the activation of the key UPR folding chaperone, binding immunoglobulin protein (BiP) (Figure 4A; Supporting Information, Figure S41). However, decreased phosphorylation of p-eIF2 $\alpha$ , increased phosphorylation of c-Jun N-terminal kinase (JNK), as well as increase of C/EBP homologous protein (CHOP) expression suggested that the damage caused by the treatment was too severe and cells were directed into cell death processes (Figure 3D).<sup>[32]</sup> Subsequently, we compared the cytotoxicity of **3met** in presence or absence of various specific UPR inhibitors, which confirmed the specific role of eIF2 $\alpha$  and JNK pathways, as well as global protein synthesis in the anticancer activity of **3met** (Figure 4B; Supporting Information, Figure S37B).

Au<sup>I</sup> and Au<sup>III</sup> complexes commonly induce UPR and ER stress.<sup>[23,33]</sup> In comparison, autophagy-inducing Au complexes are relatively rare.<sup>[26b]</sup> Autophagy ensures the self-removal of cell's own faulty material. The hallmark of the autophagy is the conversion of cytosolic LC3-I to autophagosome-bound LC3-II.<sup>[34]</sup>

We demonstrated that MDA-MB-231 cells treated with **1met** and **3met** induced dose-dependent and time-dependent conversion of LC3-I to LC3-II, indicating the activation of autophagy program (Figure 4C; Supporting Information,

## ER stress

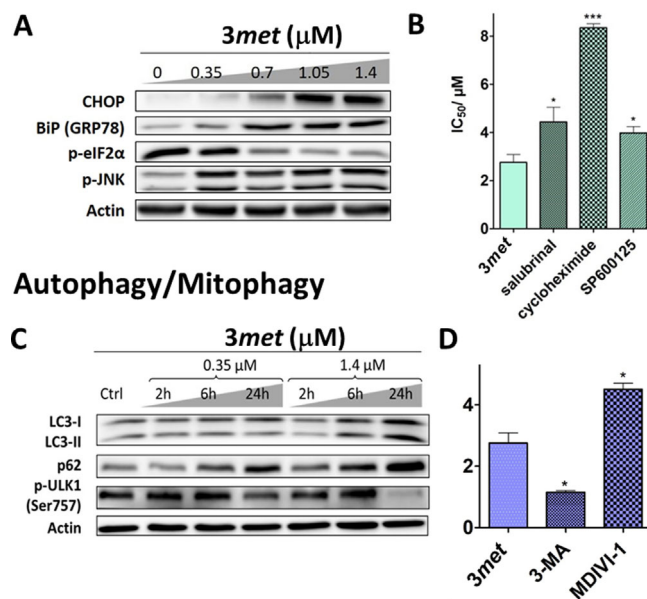


**Figure 4.** **3met**-induced inhibition of pro-survival responses. A) Western blot analysis of various proteins involved in ER stress and protein degradation in MDA-MB-231 cells treated with **3met** for 24 h at indicated concentrations. B) The cytotoxicity of **3met** upon 24 h co-incubation with salubrinal (10 μM, inhibitor of eIF2α dephosphorylation), cycloheximide (12.5 μM, inhibitor of global protein synthesis) and SP600125 (20 μM, inhibitor of JNK pathway). C) Western blot analysis of various proteins involved in autophagy in MDA-MB-231 cells treated with **3met** for 2, 6 and 24 h at indicated concentrations. D) The cytotoxicity of **3met** upon 24 h co-incubation with 3-MA (2 mM, inhibitor of autophagosome formation) and MDIVI-1 (10 μM, inhibitor of mitochondrial fission).

Figure S42). When cytotoxicity of **3met** was tested in presence of autophagy inhibitor 3-methyladenine (3-MA), it increased more than 2-fold, indicating the pro-survival role of autophagy processes (Figure 4D). Additionally, we assessed the levels of LC3-I/II and its binding protein partner, p62, in presence or absence of chloroquine (CQ), which blocks the fusion of the autophagosome with the lysosome, thereby preventing degradation of LC3-II (Supporting Information, Figure S42).<sup>[34,35]</sup> The results demonstrated that **3met** inhibited protein degradation and the accumulation of autophagosomes, leading to the impairment of pro-survival autophagic flux, which was distinctly different mechanistically from other structurally similar cyclometallated Au<sup>III</sup>-C,N complexes.<sup>[26b]</sup>

We questioned whether drug-induced mitochondrial dysfunction activated the process of mitophagy, which restore cellular mitochondrial function by clearing defective mitochondria. Selective degradation of mitochondria occurs by increasing mitochondrial fission.<sup>[36]</sup> When MDA-MB-231 cells were treated with **3met** in combination with mitochondrial fission inhibitor MDIVI-1, its cytotoxicity significantly decreased, clearly indicating the role of mitophagy in the mechanism of **3met** (Figure 4D). Notably, uncoordinated metformin was also shown to regulate mitophagy in vitro and in patients.<sup>[37]</sup>

We selected **3met**, which demonstrated the highest activity in vitro, as a lead compound for in vivo studies. To determine the maximum tolerated dose (MTD), mice were given daily *i.p.* injections of **3met** at 5, 10, 15, and 20 mg kg<sup>-1</sup> for 4 d and their body weights were monitored (Supporting Information, Figures S43). All groups of mice were bright, alert and responsive; however, transient weight loss was observed at 20 mg kg<sup>-1</sup>. The dose-limiting toxicity included kidney and liver toxicity reflected by histopathological changes (Supporting Information, Figure S45). Therefore, the MTD of **3met** for *i.p.* route was determined as 15 mg kg<sup>-1</sup>. The in vivo activity of **3met** was subsequently tested in athymic nude mice using orthotopic mammary fat pad model. Luciferase-transfected MDA-MB-231 cells were injected into 2 fat pads near pectoral nipples and 2 fat pads near inguinal nipples, and tumor growth was controlled by bioluminescent imaging (Figure 5A).<sup>[38]</sup> Mice were injected with 15 mg kg<sup>-1</sup> of **3met** or respective vehicle (DMSO in physiological saline) intraperitoneally 3 times a week on weeks 3, 4 and 5 and sacrificed on week 6. Body weight changes are shown in the Supporting Information, Figure S44. Importantly, **3met** demonstrated marked decrease of tumor burden in comparison with a vehicle-treated group and significantly slowed down the growth of quickly growing breast tumors (no growth after week 3, Figure 5B). On the contrary, the anticancer effects of uncoordinated metformin in an MDA-MB-231 mammary fat pad model were negligible even at a very high dose (250 mg kg<sup>-1</sup>).<sup>[39]</sup>

Additionally, we assessed Au biodistribution across various organs in tumor-bearing mice. Figure 5C demonstrates that **3met** selectively accumulated in tumors. The Au content in tumors was 3–5 times higher than in heart, lung, spleen, and kidneys and 3–20 times higher than in brain, liver and bone. This biodistribution pattern was very uncommon for small molecules and would be a desirable property for novel anticancer drug candidates. Subsequently, histological changes in tumor tissues were assessed by H&E staining and the effects of **3met** on tumor area and necrosis were quantified using an automated QuPath algorithm (Figure 5D–H; Supporting Information, Table S5, Figure S46). Tumors in vehicle-treated group demonstrated some areas of necrosis (10 ± 1%) caused by high proliferative activity of aggressive breast cancer cells, while drug-treated group was characterized by significant areas of necrosis (33 ± 4%), indicating anticancer effects of **3met** (Figure 5H). **3met**-treated tumors demonstrated marked inflammatory cells infiltration, indicating enhanced immune response to the primary tumor (Figure 5F). This is an important finding since basal subtypes of breast cancers that were regulated by tumor-infiltrating immune cells were linked with improved prognosis and drug sensitivity.<sup>[40]</sup>

## Discussion

Despite significant advancements in the treatment of breast cancer, TNBCs represent an unmet clinical need due to their aggressive nature and propensity to metastasize.<sup>[41]</sup> Unlike other subtypes of breast cancer, TNBCs do not



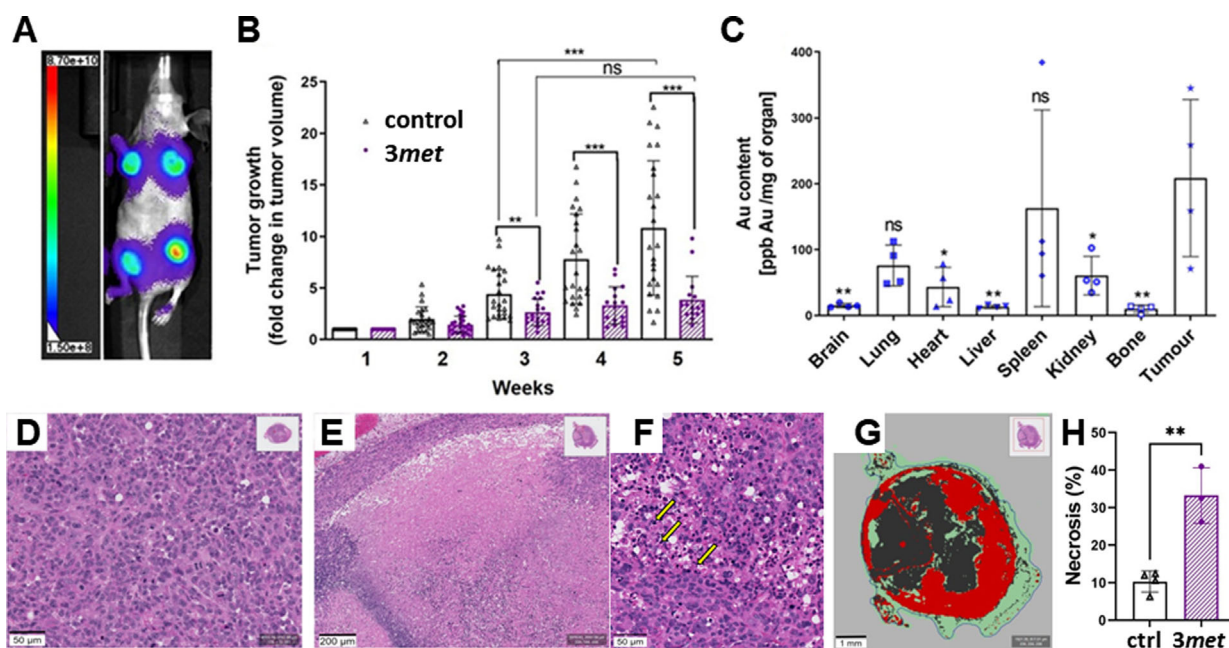


**Figure 5.** Effects of **3met** on aggressive breast tumor growth in vivo. A) Bioluminescent live image of xenografted luciferase-expressing MDA-MB-231 cells orthotopically implanted into two mammary fat pads near pectoral and inguinal nipples. Post-implantation week 5. B) Growth of MDA-MB-231 tumors from week 1 (before treatment) presented as a fold change in tumor volume. Starting from week 2 tumors became palpable and their volume was measured by calliper weekly. Mice ( $n=7$ ) were treated with **3met** at  $15 \text{ mg kg}^{-1}$  or respective vehicle (DMSO in sterile saline) via *i.p.* route every other day on weeks 3, 4 and 5. C) Au accumulation in mouse organs obtained from **3met**-treated mice at the endpoint and quantified by ICP-MS. D) Representative H&E-stained tumor tissue of a vehicle-treated mouse, demonstrating grade 3 breast carcinoma with high rate of mitosis. E and F) Representative H&E-stained tumor tissues of a **3met**-treated mouse, demonstrating (E) wide area of necrosis and strong lymphohistiocytic tumor infiltration and (F) lymphohistiocytic infiltration (depicted with yellow arrows). G) Algorithm for quantification of tumor tissues using QuPath software (random trees pixel classifier, red color is tumor, black is necrosis and green is stroma). H) Quantification of necrosis in H&E-stained tumor tissues of vehicle- and **3met**-treated mice using algorithm presented in (F). Statistical analysis was performed by one-way ANOVA test with (B) Bonferroni or (C) Dunnett post hoc analysis (vs. tumor) or (B, H) unpaired T test using GraphPad Prism 9 software (GraphPad Software Inc., CA) with  $p < 0.05$  considered as significant (\*  $p < 0.05$ , \*\*  $p < 0.01$ , \*\*\*  $p < 0.001$ , ns: not significant).

express estrogen, progesterone and Her2 receptors and cannot be treated with hormone therapies or Her2-targeting drugs, such as Trastuzumab. Therefore, the only systemic treatment that can be used for TNBCs is chemotherapy. It is known that TNBCs readily respond to currently used chemotherapeutic options, for example, ACT regimen (anthracycline, cyclophosphamide and taxane);<sup>[42]</sup> however, despite initial response, they quickly relapse and metastasize, which poses a serious challenge for the selection of second-line treatment options. In recent years, several classes of metal-based compounds have been developed as anticancer therapeutic agents endowed with multimodal activity against TNBCs in vitro and in vivo.<sup>[43]</sup> In this context, we further explored the potential of organometallic chemistry, designing a new series of TNBC-targeting cyclometalated Au<sup>III</sup> prodrug complexes designed to deliver metformin.

The phenotypic aggressiveness of TNBCs is related to their dependency on glucose and lipids,<sup>[44]</sup> which cancer cells use for production of energy. It was previously shown that antidiabetic drug metformin targeted glucose metabolism in TNBCs,<sup>[45]</sup> which made this drug particularly toxic to this group of breast cancers. However, the use of metformin for the treatment of TNBCs is hindered by its inability to effectively penetrate through cellular membranes. The approach detailed in this study was based on the conjugation of

metformin and phenformin with Au<sup>III</sup> pharmacophores, resulting in synergistic mitochondrial damage. We hypothesized that cyclometalated Au<sup>III</sup> scaffolds can act as multimodal prodrugs achieving targeted release of metformin and phenformin. To test this approach, we prepared a series of cyclometalated Au<sup>III</sup> complexes of metformin and phenformin and investigated their potential for treatment of TNBCs. The release of metformin was dictated by the cyclometalated fragment with the most cytotoxic complex **3met** being the most efficient amongst the panel of compounds tested. **3met** also displayed nanomolar cytotoxic activities and was about 28-fold more active than cisplatin in MDA-MB-231 cells (TNBC/basal breast cancer cell line) and more than 6000-fold cytotoxic than free metformin. **3met** was also markedly more active than its cyclometalated precursor **3**.

We demonstrated that Au<sup>III</sup> pharmacophores and metformin displayed synergistic action and completely shut down energy production in TNBC cells. A number of prodrugs utilize the Warburg effect<sup>[46]</sup> to switch cancer cell metabolism from glycolysis to oxidative phosphorylation.<sup>[28a,47]</sup> In contrast, **3met** fully inhibited mitochondrial respiration, thereby forcing cancer cells to increase glucose production via glycolysis (Figure 3 A and B). However, prolonged exposure to high concentrations of **3met** resulted in a severe energetic crisis leading to the failure of breast cancer cells to protect

themselves by metabolic reprogramming, as well as other prosurvival programs, such as UPR and autophagy. Specifically, **3met** interfered with the process of mitophagy, aimed to clear the defective mitochondria following drug-induced mitochondrial damage (Figure 4D). To the best of our knowledge, this is the first example of a Au complex, which not only interfered with the normal mitochondrial function and protein homeostasis in cancer cells, but also thwarted their attempts to restore normal cellular function.

Encouraged by the anticancer potential of **3met**, we tested the efficacy of this drug candidate in an orthotopic mammary fat pad model in athymic nude mice, where MDA-MB-231 cells were implanted into 4 nipples, simultaneously forming 4 aggressive breast tumors (Figure 5). In this model, implanted cancer cells match the tumor histotype of the organ, thereby providing a more realistic disease-relevant environment in contrast to commonly used xenograft models. **3met** significantly reduced tumor burden in comparison to vehicle-treated mice and no tumor growth was observed after week 3. Based on these findings, we believe that **3met** is an effective metformin prodrug, which was able to slow the growth of invasive TNBC with subsequent activation of immune system by targeting the dependency of this cancer subtype on energy production.

## Conclusion

We designed a new series of Au<sup>III</sup> complexes, featuring both energy-disrupting metformin or phenformin ligands and multitarget Au<sup>III</sup> species. In vitro evidence demonstrated that metabolic changes caused by **3met** initiated attempts of cancer cells to protect themselves by metabolic reprogramming, UPR and mitophagy. These defense processes were successfully prevented by shutdown of mitochondrial respiration and impairment of autophagic flux, leading to the inhibition of protein degradation and apoptotic cell death. High degree of selectivity of the novel complexes to cancer cells over healthy cells were observed. Lead drug candidate **3met** halted the growth of aggressive breast tumors in a mammary fat pad breast cancer model and activated the immune response, indicating the potential benefits of this drug candidate for TNBC patients with high risk of metastasis and relapse.

## Acknowledgements

The work described in this paper was funded by Ministry of Education Singapore (MOE2018-T2-1-139 to W.H.A.). M.V.B. acknowledges financial support from City University of Hong Kong (Project No. 7200682 and 9610518). I.V.B. acknowledges support from the Lynn Sage Cancer Research Foundation. M.V.B. acknowledges Tibor Hajsz for generating the artworks and Siti Nuraisyah Bte Nordin for help with Seahorse experiments. A.C. acknowledges Cardiff University for funding. This work was also supported by the Northwestern University the Center for Advanced Microscopy and the Mouse Histology and Phenotyping Laboratory supported by

NCI P30-CA060553 awarded to the Robert H Lurie Comprehensive Cancer Center. P.R. acknowledges financial support from Slovak Grant Agencies APVV (grant APVV-19-0024) and VEGA (grant 0504/20).

## Conflict of interest

M.V.B., I.V.B., and W.H.A. are co-inventors of a patent application related to this work.

**Keywords:** antitumor agents · drug discovery · metabolism · metformin · prodrugs

- [1] N. A. Kasim, M. Whitehouse, C. Ramachandran, M. Bermejo, H. Lennernaes, A. S. Hussain, H. E. Junginger, S. A. Stavchansky, K. K. Midha, V. P. Shah, G. L. Amidon, *Mol. Pharm.* **2004**, *1*, 85–96.
- [2] a) F. Zi, H. Zi, Y. Li, J. He, Q. Shi, Z. Cai, *Oncol. Lett.* **2018**, *15*, 1–8; b) J. M. Evans, L. A. Donnelly, A. M. Emslie-Smith, D. R. Alessi, A. D. Morris, *Br. Med. J.* **2005**, *330*, 1304–1305; c) M. Bodmer, C. Meier, S. Krahenbuhl, S. S. Jick, C. R. Meier, *Diabetes Care* **2010**, *33*, 1304–1308.
- [3] a) S. Andrzejewski, S.-P. Gravel, J. St-Pierre, M. Pollak, *Cancer Metab.* **2014**, *2*, 12; b) M. Cazzaniga, B. Bonanni, *BioMed Res. Int.* **2015**, 972193.
- [4] a) D. Hanahan, R. A. Weinberg, *Cell* **2000**, *100*, 57–70; b) D. Hanahan, R. A. Weinberg, *Cell* **2011**, *144*, 646–674.
- [5] a) Y. Zhang, J.-M. Yang, *Cancer Biol. Ther.* **2013**, *14*, 81–89; b) F. Bost, A. G. Decoux-Poullot, J. F. Tanti, S. Clavel, *Oncogenesis* **2016**, *5*, e188.
- [6] S. Jin, R. S. DiPaola, R. Mathew, E. White, *J. Cell Sci.* **2007**, *120*, 379–383.
- [7] H. R. Bridges, A. J. Y. Jones, M. N. Pollak, J. Hirst, *Biochem. J.* **2014**, *462*, 475–487.
- [8] M. Zakikhani, R. Dowling, I. G. Fantus, N. Sonenberg, M. Pollak, *Cancer Res.* **2006**, *66*, 10269–10273.
- [9] R. Rattan, R. P. Graham, J. L. Maguire, S. Giri, V. Shridhar, *Neoplasia* **2011**, *13*, 483–491.
- [10] I. Ben Sahra, K. Laurent, S. Giuliano, F. Larbret, G. Ponzio, P. Gounon, Y. Le Marchand-Brustel, S. Giorgetti-Peraldi, M. Cormont, C. Bertolotto, M. Deckert, P. Auberger, J.-F. Tanti, F. Bost, *Cancer Res.* **2010**, *70*, 2465–2475.
- [11] Y. Li, M. Wang, P. Zhi, J. You, J.-Q. Gao, *Oncotarget* **2018**, *9*, 2158–2174.
- [12] H. A. Hirsch, D. Iliopoulos, P. N. Tsiachlis, K. Struhl, *Cancer Res.* **2009**, *69*, 7507–7511.
- [13] S. Jiralerspong, S. L. Palla, S. H. Giordano, F. Meric-Bernstam, C. Liedtke, C. M. Barnett, L. Hsu, M.-C. Hung, G. N. Hortobagyi, A. M. Gonzalez-Angulo, *J. Clin. Oncol.* **2009**, *27*, 3297–3302.
- [14] G. G. Graham, J. Punt, M. Arora, R. O. Day, M. P. Doogue, J. K. Duong, T. J. Furlong, J. R. Greenfield, L. C. Greenup, C. M. Kirkpatrick, J. E. Ray, P. Timmins, K. M. Williams, *Clin. Pharmacokinet.* **2011**, *50*, 81–98.
- [15] S. Salpeter, E. Greyber, G. Pasternak, E. Salpeter, *Arch. Intern. Med.* **2003**, *163*, 2594–2602.
- [16] D. W. Proctor, J. M. Stowers, *Br. Med. J.* **1967**, *4*, 216.
- [17] M. Cetin, S. Sahin, *Drug Delivery* **2016**, *23*, 2796–2805.
- [18] G. Cheng, J. Zielonka, O. Ouari, M. Lopez, D. McAllister, K. Boyle, C. S. Barrios, J. J. Weber, B. D. Johnson, M. Hardy, M. B. Dwinell, B. Kalyanaraman, *Cancer Res.* **2016**, *76*, 3904–3915.
- [19] K. M. Huttunen, A. Mannila, K. Laine, E. Kempainen, J. Leppanen, J. Vepsalainen, T. Jarvinen, J. Rautio, *J. Med. Chem.* **2009**, *52*, 4142–4148.



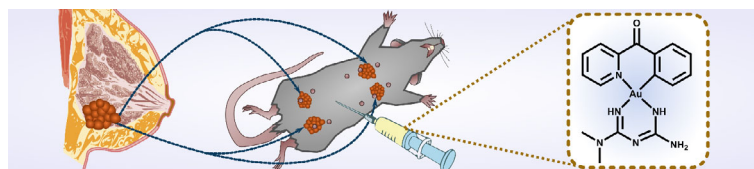
## Research Articles



## Antitumor Agents

M. V. Babak,\* K. R. Chong, P. Rapta,  
M. Zannikou, H. M. Tang, L. Reichert,  
M. R. Chang, V. Kushnarev, P. Heffeter,  
S. M. Meier-Menches, Z. C. Lim, J. Y. Yap,  
A. Casini, I. V. Balyasnikova,  
W. H. Ang\* ■■■■-■■■■

Interfering with Metabolic Profile of  
Triple-Negative Breast Cancers Using  
Rationally Designed Metformin Prodrugs



Au<sup>III</sup> prodrugs of anti-diabetic medicines metformin and phenformin were developed. These compounds effectively decreased triple negative breast tumor burden. The mode of action of novel complexes was linked to energetic crisis

and abolishment of pro-survival responses leading to irreversible cell death.